Evaluation of X-Band Polarimetric-Radar Estimates of Drop-Size Distributions From Coincident S-Band Polarimetric Estimates and Measured Raindrop Spectra

Marios N. Anagnostou, *Member, IEEE*, Emmanouil N. Anagnostou, Gianfranco Vulpiani, *Member, IEEE*, Mario Montopoli, Frank S. Marzano, *Senior Member, IEEE*, and Jothiram Vivekanandan

***Abstract*—Recent research has demonstrated the value of polarimetric measurements for the correction of rain-path attenuation at X-band radar frequency and the estimation of rain parameters including drop-size distributions (DSD). The issue this paper is concerned with is to what degree uncertainties in attenuation correction can affect the estimation of DSD. Since attenuation-correction uncertainty enhances with rain path, our hypothesis is that DSD retrieval uncertainty at X-band may deteriorate with range. In this paper, we evaluate the relative accuracy of X-band DSD retrieval against DSD estimates from S-band radar observations and *in situ* disdrometer spectra. We present comparisons of various techniques for estimating DSD model parameters from attenuation-corrected X-band dual-polarization radar data. Coincident X-band polarimetric-radar (XPOL) and S-band polarimetric-radar dual-polarized radar measurements from the International H_2O Project experiment as well as coincident XPOL (MP-X) measurements over disdrometer during a typhoon storm case in Japan are used to assess the accuracy of the different DSD retrieval algorithms applied to X-band radar measurements.**

***Index Terms*—Attenuation correction, drop-size distribution (DSD) retrievals, polarimetric radar, S-band radar, X-band radar.**

I. Introduction

THE LACK of detailed knowledge of drop-size distribution (DSD) is the primary factor that limits the accuracy of radar and satellite rain retrievals. The relation between radar reflectivity and rain rate can be analytically estimated only if the DSD is specified. Hence, various rain-rate estimators are derived using multiple polarimetric-radar observations, i.e., horizontal reflectivity ($Z_{\rm H}$ in decibels of Z), differential reflectivity ($Z_{\rm DR}$ in decibels), and the slope of the differential-propagation phase shift ($K_{\rm DP}$ in degrees per kilometer) that are related to DSD [9]. In addition, understanding and characterization of precipitation microphysics is required to improve parameterizations in numerical-weather-prediction models [25], [32]. The rain DSD could relate in bulk-sense microphysical processes of evaporation, accretion, and precipitation rate, together with vertical air motion.

Extensive research based on measured DSD spectra suggests that, for short time periods proportionate with radar measurements, DSDs are more typically represented by a gamma distribution [28]

$$N(D) = N_0 D^{\mu} \exp(-\Lambda D) \tag{1}$$

where N_0 ($\mathrm{m}^{-3}\mathrm{mm}^{-\mu-1}$) is the concentration-number parameter, μ is the distribution-shape parameter, Λ (in per millimeter) is the slope term, and D (in millimeters) is the equivalent volume drop diameter. Note the following: 1) Specific attention should be yield to the total number concentration and 2) (1) reduces to the exponential model of Marshall and Palmer [16] when $\mu = 0$. The slope parameter Λ relates to the characteristic size of the raindrops such as the mean diameter [$\langle D \rangle = (2/\Lambda)$] or median volume diameter

$$\Lambda D_0 \cong 3.67 + \mu. \tag{2}$$

Most of these were focused on estimating D_0 and/or the N_0 but not all three parameters that characterize the gamma distribution. Most of the current rainfall DSD retrieval techniques are focused on cases with none to moderate attenuation (S-/C-band frequency) radar-frequency observations.

Several techniques have been proposed to estimate the governing gamma DSD model parameters in rainfall from radar measurements [6], [8], [10], [18], [26]. The method by Gorgucci *et al.* [10]–[12], which was proposed for C-band, and a similar technique by Bringi *et al.* [8], which was developed for S-band frequency, estimate the three parameters

Manuscript received October 15, 2007; revised February 16, 2008. Current version published October 1, 2008. This work was supported by the EU Marie Curie Excellence Grant Project PreWEC under Grant MEXT-CT-2006-038331.

M. N. Anagnostou is with the Institute of Inland Waters, Hellenic Center for Marine Research, 19013 Anavissos, Greece (e-mail: managnostou@ath.hcmr.gr).

E. N. Anagnostou is with the Institute of Inland Waters, Hellenic Center for Marine Research, 19013 Anavissos, Greece, and also with the Department of Civil and Environmental Engineering, University of Connecticut, Storrs, CT 06269 USA.

G. Vulpiani is with Italian Department of Civil Protection, 00189 Rome, Italy (e-mail: gianfranco.vulpiani@protezionecivile.it).

M. Montopoli is with Center of Excellence CETEMPS—Department of Electrical Engineering and Information Engineering, University of L'Aquila, 67040 L'Aquila, Italy.

F. S. Marzano is with Center of Excellence CETEMPS—Department of Electrical Engineering and Information Engineering, University of L'Aquila, 67040 L'Aquila, Italy, and also with the Department of Electronic Engineering and Center of Excellence CETEMPS, University of Rome "La Sapienza," 00184 Roma, Italy.

J. Vivekanandan is with the National Center for Atmospheric Research, Boulder, CO 80303 USA.

Digital Object Identifier 10.1109/TGRS.2008.2000757

of the gamma distribution by utilizing the two power-related radar parameters ($Z_{\rm H}$ and $Z_{\rm DR}$) and the $K_{\rm DP}$ (in degrees per kilometer). Park *et al.* [22] adapted a similar method for use at the X-band frequency to estimate D_0 (in millimeters) and the "intercept" parameter N_W (in $\rm m^{-3}mm^{-1}$), which is the N_0 of an equivalent exponential DSD that has the same liquid water content (in grams per cubic meter) and D_0 (in millimeters) as the normalized gamma DSD [10]. Other recent studies have proposed the estimation of one of the DSD parameters as part of attenuation correction and/or rain estimation. Matrosov *et al.* [18] estimated D_0 by relating it with the attenuation-corrected $Z_{\rm DR}$ for X-band, while the technique developed by Testud *et al.* [26] provides estimates of N_W for C-/X-band frequencies using an attenuation-correction algorithm that devices the differential phase shift ($\Phi_{\rm DP}$ in degrees) as an external constraint to the attenuation-estimation method. The methods aforementioned are either two- or three-parameter physical-based *ad hoc* or empirical algorithms. There is also a nonparametric estimation of DSD from slant-profile dual-polarized Doppler spectra observations presented by Moisseev *et al.* [19], [20]. Vulpiani *et al.* [30] has developed a nonparametric approach to estimate the three governing parameters of DSD from S- or C-band dual-polarization radar parameters on the basis of a regularized artificial neural network (NN).

This paper focuses on the comparison and evaluation of X-band versus S-band DSD-parameter retrievals, for different radar retrieval techniques, and on the assessment of their performance against measured raindrop spectra. The first part of this paper describes the basic algorithms used to retrieve the DSD by means of polarimetric-radar measurements. The second part will assess the retrieval algorithms based on coincident X-/S-band polarimetric-radar observations and X-band measurements over *in situ* disdrometer observations. The question this paper aims to address is to what degree uncertainties in X-band attenuation correction can affect the estimation of gamma DSD parameters at this frequency. Since attenuation-correction uncertainty enhances with rain path, our hypothesis is that X-band DSD retrieval uncertainty would potentially deteriorate with increasing range [1], [2], [27].

II. Experimental Data

This paper uses data from two experiments. In the first one, we use coincident X-/S-band low-elevation observations from the 2002 International H_2O Project (IHOP) in western Oklahoma to statistically quantify the uncertainty in the X-band DSD retrieval. In the second and third experiments, we use coincident radar and disdrometer measurements taken in Japan during the pass of a typhoon storm and from an urban setting in Athens, for the evaluation of the algorithms with ground-truth measurements.

In IHOP, the National Observatory of Athens X-band polarimetric radar (XPOL) was deployed a few meters from NCAR's S-band polarimetric radar (S-Pol), and the two radars were operated at closely matched scanning strategies. During storm development, multiple-elevation plan-position-indicator sector scans and range-height-indicator scans were conducted. For the objectives of this paper, two major storm events on May 17, 2002 and June 16, 2002 that were measured simultaneously by the two radars were selected for analysis. XPOL measurements were corrected for rain-path attenuation as described in [1]. Sample comparisons of simulated (from S-Pol observations) versus XPOL-measured and attenuation-corrected profiles of $Z_{\rm H}$ and $Z_{\rm DR}$ parameters are shown in Fig. 1. The method used for the DSD retrievals from S-Pol observations, which were then used for the X-band simulations, is described in [6]. The profiles show strong range-dependent bias in the raw XPOL data and an adequate adjustment by the attenuation-correction technique.

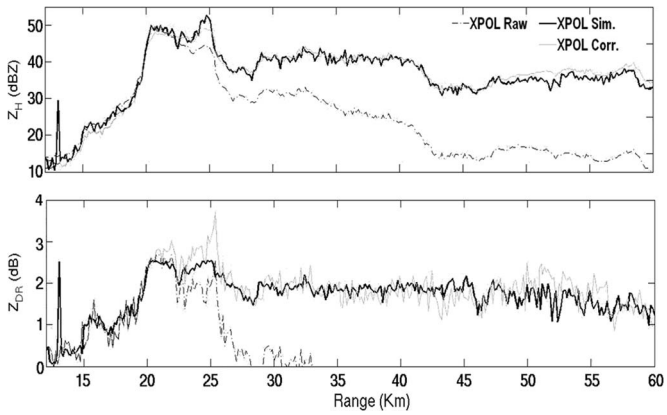

Fig. 1. Sample $Z_{\rm H}$ and $Z_{\rm DR}$ ray profiles of XPOL raw/attenuation-corrected and XPOL parameters simulated (from S-Pol observations) parameters.

The second data set is associated with a maritime convective regime in Japan. It includes radar and disdrometer data from Ebina (35.4° N, 139.4° E), Japan, where the National Research Institute for Earth Science and Disaster Prevention (NIED) is operating a dual-polarization and Doppler X-band radar (named MP-X) [15]. For the validation of MP-X, there is a network of *in situ* stations that consists of four rain gauges and three Joss–Waldvogel (JWD)-type disdrometers at approximate 10-km intervals along an azimuth of about 257°. The MP-X radar data were quality controlled [22] and corrected for rain-path attenuation using the algorithm described in [1]. The drop spectra were collected every minute and processed using quality-control procedures described in [22]. A correction was applied for the dead-time effect that can cause underestimation of small drops [23]–[31]. The T-matrix approach [4] was employed to simulate radar parameters on the basis of drop spectra. In this paper, we used about 17 h of coincident MP-X and JWD measurements from one of the sites (∼18-km range from the radar) during the passage of a typhoon on August 9, 2003. As shown in Fig. 2, both the disdrometer and radar measured high (40–55 dBZ) to moderate (30–40 dBZ) reflectivities during this storm passage. As noted in the figure, MP-X measurements are well correlated with simulated parameters by JWD. There are no systematic differences indicating unbiased radar measurements.

III. Review of the DSD Retrieval Techniques

This paper is using theoretical generated DSD spectra in rain to estimate the coefficients of the three (constrained, β, and NN)

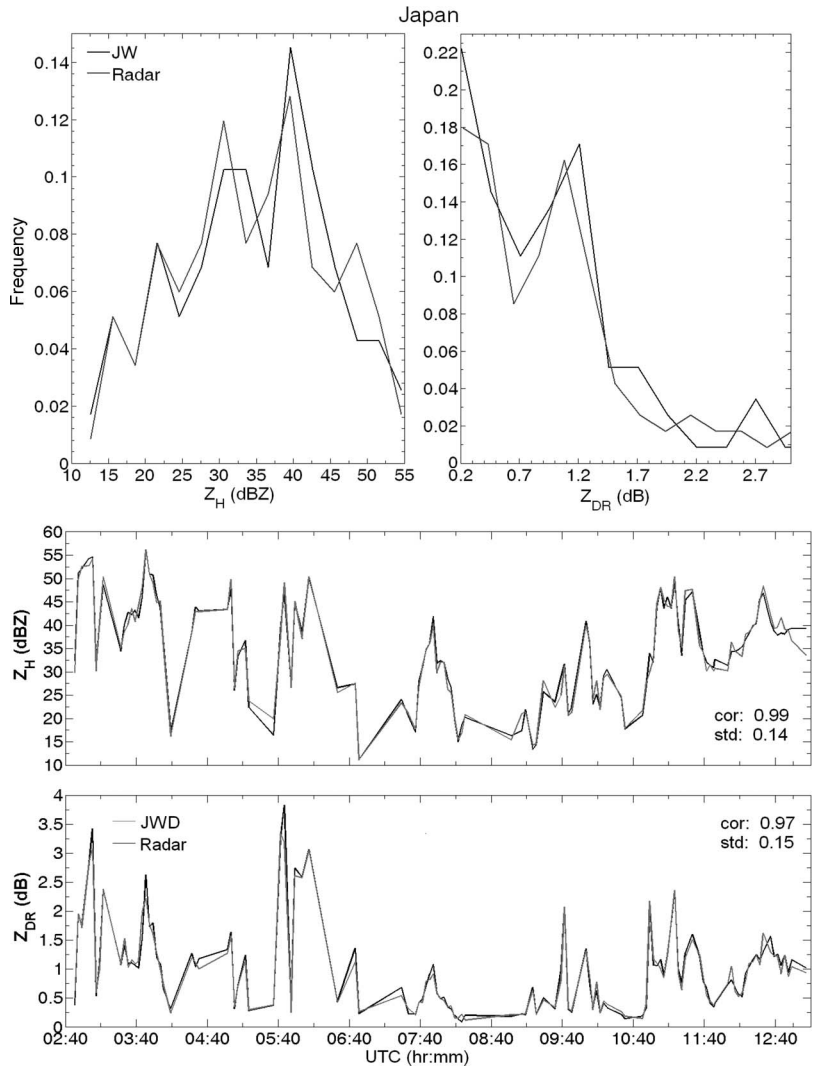

Fig. 2. (Upper panel) Relative frequency and (lower panel) collocated sample time-series plots of $Z_{\rm H}$ and $Z_{\rm DR}$ from MP-X and the JWD-type disdrometer in Japan.

algorithms. The scattering simulations performed using T-matrix [4] are based on the following assumptions: polynomial [6] raindrop axis ratio for the constrained- and NN-method linear [13] axis ration for the β method and hydrometeor temperature of 20°. The radar parameters were computed for widely varying DSDs by randomly choosing the uniformly distributed N_W, D_0, and μ parameters over the following ranges: $2 \leq N_W \leq 5$ (N_W in $\rm m^{-3}mm^{-1}$), $0.5 < D_0 < 3.5$ (D_0 in millimeters), and $-1 < \mu < 11$, with the following constraint of $Z_{\rm H} < 55$ dBZ, $R < 300$ mm $\rm h^{-1}$, and $N_T \leq 10^4$.

A. Constrained Method

This method is based on the premise that the governing parameters of the gamma DSD model are not mutually independent. This aspect can be of great significance, because it can help to reduce the number of unknowns, thus enable the retrieval of the DSD parameters from a pair of more independent radar measurements, i.e., the $Z_{\rm H}$ and $Z_{\rm DR}$. Analysis of the theoretically generated DSD spectra revealed a high correlation between the shape-size relation μ of the gamma distribution and the slope Λ (in per millimeter), which led to the derivation of an empirical μ–Λ relation

$$\Lambda\left(\frac{1}{\rm mm}\right) = 0.0136\,\mu^2 + 0.6984\,\mu + 1.513. \qquad (3)$$

A point to note is that the validity of this method is still under debate, since studies by Moisseev and Chandrasekar [20] and Ulbrich and Atlas [29] have argued that the correlation of the μ–Λ relation does not represent physics because of (2) relation and that (3) is valid on a particular range of D_0 [3] values and not for its whole spectrum.

The method starts with the estimation of median drop diameter D_0 (in millimeters) and the interception parameter N_W (where N_W is in $\rm m^{-3}mm^{-1}$) from attenuated corrected X- or S-band radar parameters ($Z_{\rm Hmm}$ in $\rm mm^6m^{-3}$ and $Z_{\rm DR}$ in decibels) based on relationships derived from T-matrix [4] scattering calculations using the axial-ratio model [5]

$$D_0({\rm mm}) = \alpha_1 Z_{\rm DR}^3 + \alpha_2 Z_{\rm DR}^2 + \alpha_3 Z_{\rm DR} + \alpha_4 \qquad (4)$$

$$N_W({\rm m^{-1}mm^{-3}}) = \log_{10}(10^b Z_{\rm H_{mm}} 10^{b_1 Z_{\rm DR}^2 + b_2 Z_{\rm DR}}) \qquad (5)$$

while the shape parameter μ can then be determined by using (2) and minimizing (with respect to μ) the least squares difference of calculated versus observed drop counts over a range of drop-diameter bins.

B. β Method

The method treats the raindrop shape–size relations as a variable according to the linear raindrop axis ratio (r) to drop-size relationship shown as follows

$$r = 1.03 - \beta D. \tag{6}$$

The method starts with the estimation of the β parameter using a nonlinear-regression approach described by Gorgucci *et al.* [14] for scattering simulations performed for X-band (or S-band) frequency

$$\beta = c\left(\frac{K_{\rm DP}}{Z_{\rm Hmm}}\right)^{C_1} \xi_{\rm DR}^{C_2} \tag{7}$$

where $\xi_{\rm DR} = 10^{0.1 Z_{\rm DR}}$ is the differential reflectivity in linear units. Incorporating the β term, the expression that can be derived for the N_W and D_0 were

$$D_0 = c_3\left(\frac{\xi_{\rm DR} - 0.8}{\beta}\right)^{C_4} \tag{8}$$

$$N_W = c_5\left(\frac{\xi_{\rm DR} - 0.8}{\beta}\right)^{C_6} Z_{\rm Hmm}^{C_7} \tag{9}$$

where N_W is the normalized gamma-intercept parameter [10] given in per cubic meter per millimeter ($\rm m^{-3} \cdot mm^{-1}$). Due to significant uncertainty in estimating μ with this method [8], this parameter is not estimated by β method. To avoid any noise contamination from $K_{\rm DP}$ in the DSD retrievals, we set as 0.10° $\rm km^{-1}$ and 10 dBZ, the lower $K_{\rm DP}$ and $Z_{\rm H}$ thresholds, respectively, for applying this method.

C. NN Method

The last method tested herein is an artificial NN algorithm proposed in [30]. It is a nonlinear parameterized mapping from an input x to an output $y = NN(x; w, M)$, where w is the vector of parameters relating the input to the output, while the functional form of the mapping (i.e., the architecture of the NN) is denoted as M. The multilayer preceptor architecture, considered here, is a mapping model composed of several layers of parallel processors (i.e., neurons). For the training of the network, it used the so-called supervised learning method with a training set $D = (x_i, t_i)$ of inputs and targets. In this paper, the NN method uses a three-input configuration ($Z_{\rm H}$, $Z_{\rm DR}$, and $K_{\rm DP}$)

$$D_0({\rm mm}) = f(Z_{\rm H}, Z_{\rm DR}, K_{\rm DP}) \tag{10}$$

$$N_W = f(Z_{\rm H}, Z_{\rm DR}, K_{\rm DP})({\rm m^{-3} \cdot mm^{-1}}) \tag{11}$$

$$\mu = f(Z_{\rm H}, Z_{\rm DR}, D_0) \tag{12}$$

TABLE I
(a) COEFFICIENT VALUES OF THE CONSTRAINED ALGORITHM PARAMETERIZATIONS [(4) AND (5)] FOR THE X- AND S-BAND RADAR FREQUENCIES. (b) COEFFICIENT VALUES OF THE β ALGORITHM PARAMETERIZATIONS [(7)–(9)] FOR THE X- AND S-BAND RADAR FREQUENCIES (COEFFICIENTS TAKEN AS IS FROM [14])

Band/Coefficient	*a1*	*a2*	*a3*	*a4*	*b*	*b1*	*b3*
S (3 GHz)	0.141	-0.857	1.956	0.538	1.724	0.40	-2.40
X (9.3 GHz)	0.044	-0.286	1.195	0.626	1.610	0.198	-1.74

(a)

Band/Coefficient	*c*	*c1*	*c2*	*c3*	*c4*	*c5*	*c6*	*c7*
S (3 GHz)	1.594	0.342	1.155	0.172	1.019	7.951	-0.654	0.079
X (9.3 GHz)	0.536	0.276	1.212	0.202	0.884	7.030	-0.581	0.083

(b)

where $Z_{\rm H}$ in decibels of Z, $Z_{\rm DR}$ in decibels, and $K_{\rm DP}$ in degrees per kilometer.

For the S-Pol DSD retrievals, the same theoretical generated DSD parameters have been used to simulate the radar parameters at S-band frequency to estimate the coefficients of the three earlier DSD retrieval algorithms. The algorithm coefficients for constrained and β method for S-/X-band radar frequencies are shown in Table I(a) and (b).

IV. EVALUATION OF THE ALGORITHMS

A. Radar/Disdrometer Comparisons

In this section, we use coincident data sets from radar and *in situ* disdrometer measurements to evaluate the different DSD retrieval algorithms. Specifically, we use as input X-band dual-polarization radar parameters corrected for rain-path attenuation and compare estimates from the algorithms in corresponding DSD parameters (N_W, D_0, and μ) derived from measured raindrop spectra. Evaluation is performed based on visual-inspection and statistical-comparison methods. Visual inspection includes time-series plots that are used to show the covariation of the technique estimates in comparison to the corresponding parameters derived from disdrometer-measured raindrop spectra. The statistical methods include the bias, correlation coefficient, and relative root mean-square difference (rRMSE) of the retrieved from radar parameters (hereafter, named estimated) versus the disdrometer-derived (hereafter, named reference) DSD parameter (N_W, D_0, and μ). The bias is defined as the ratio of total estimated to total reference rainfall, while rRMSE is the RMS normalized by the reference mean value. Visual and statistical comparisons are discussed next.

Fig. 3 shows the time series of the three governing DSD parameters ($\log 10 N_W$, D_0, and μ) estimated from the three different retrieval algorithms using actual radar (MP-X) measurements as compared to DSD parameters determined from raindrop (JWD) spectra. Table II shows the corresponding bulk statistics of the three radar algorithms on the basis of comparisons with the disdrometer-derived DSD parameters. The figure shows a good agreement between all three algorithm retrievals

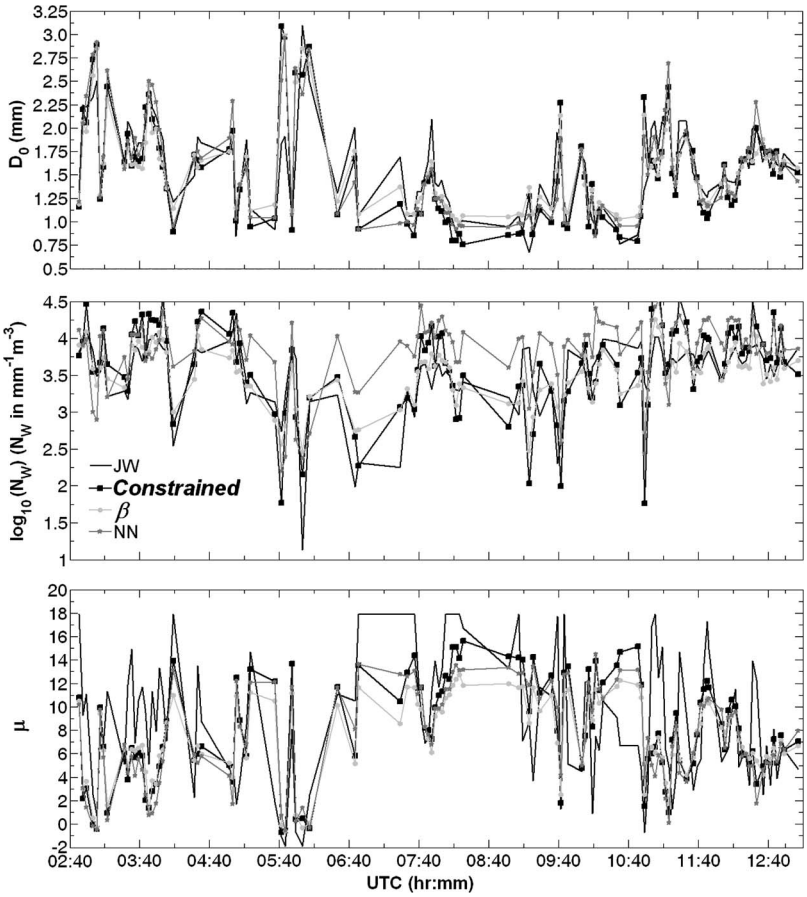

Fig. 3. Time-series plot of the three governing DSD parameters (N_W, D_0, and μ) estimated from the three different retrieval algorithms (NN, constrained, and β) using actual radar (MP-X) parameters as compared to DSD parameters determined from raindrop (JWD-type disdrometer) spectra.

TABLE II
BULK STATISTICS COMPARING RADAR ESTIMATES FROM THE THREE METHODS WITH DISDROMETER (JWD-TYPE DISDROMETER) MEASUREMENTS FROM JAPAN AND RADAR RETRIEVALS FROM ACTUAL RADAR MEASUREMENTS (MP-X)

NN | *constrained* | *β*	*Correlation*	*Bias*	*rRMS*
D_0	0.86 | 0.88 | 0.82	0.99 | 0.96| 0.99	0.17 | 0.19 | 0.16
N_W	0.63 | 0.76 | 0.76	1.09 | 1.02| 0.99	0.12 | 0.10 | 0.09
μ	0.44 | 0.47 | 0.46	0.84 | 0.89 | 0.86	0.60 | 0.57 | 0.53

and disdrometer-derived values in terms of D_0. We particularly note the adequate catch from all methods of the peak of the D_0 value at about 06:00 UTC. The β and the constrained method exhibit good agreement with the disdrometer-derived values, but the NN, although well correlated, systematically overestimates the disdrometer-derived N_W values by about 9%. This is most apparent between 06:00 and 09:30 UTC, indicating a weakness possibly due to the use of $K_{\rm DP}$ measurements in moderate-to-low rainfall, something that it is not noted with the β method. Even though, there are arguments that estimation of the slope of axial ratio (β) of raindrop introduces some errors due to the weakness of the linear axial-ratio model to catch the distribution of small drops [33], the algorithm exhibit good agreement. Compare to the NN algorithm, this is probably because the β method does not use the $K_{\rm DP}$ as input to the equations that estimate the D_0 or N_W, as NN algorithm does. In terms of μ, all algorithms exhibit similar results to each other, but the performance is generally weaker to the disdrometer-derived values, compared to the other two DSD parameters (N_W and D_0). Something that should be noticed here is that all three methods estimate μ based on the generic constrained μ–Λ [(3)] and ΛD_0 (μ) [(2)] relations.

A point to note is that the disdrometer data were 3-min averages, which was done to reduce the noise in the measurements, and that the bulk statistics presented in Table II were calculated for $Z_{\rm H}$ and $K_{\rm DP}$ values greater than 10 dBZ and 0.1° km^{-1}, respectively.

B. S-Pol/XPOL Comparison

Several (∼100) coincident rays of joint XPOL/S-Pol observations with significant rain-path attenuation were selected from the two major storm cases in IHOP to statistically quantify the performance of the XPOL DSD-parameter retrievals relative to S-Pol. In Fig. 4, we show a sample ray profile from the database. From left to right, we show the NN-, constrained-, and β-method algorithm estimates of D_0 (upper), N_W (middle), and μ parameters. In the bottom right, we show the reflectivity profile for this ray measured by XPOL (rain-path-attenuation corrected based on the algorithm by Anagnostou *et al.* [1])

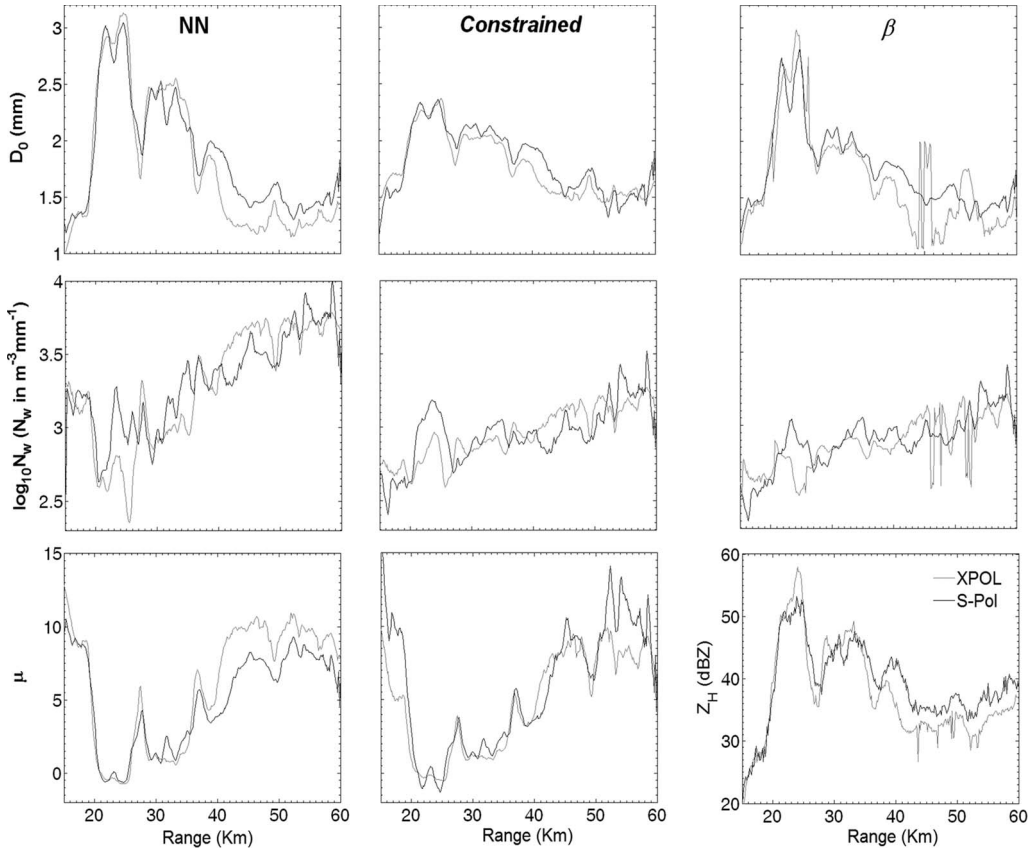

Fig. 4. (Left panels) Sample ray plot of gamma DSD parameters estimated by NN, (middle panels) constrained, and (right panels) β method. The bottom right panel shows the $Z_{\rm H}$ ray profile from attenuation-corrected XPOL and S-Pol data.

and S-Pol. Our overall observation from the sample ray case is that X-band retrievals exhibit good agreement with the S-band estimates using corresponding algorithms. A point to note is that the NN exhibits closer agreement between X- and S-band estimates relative to the other algorithms (particularly in the convective regime) but larger small-scale variability relative to the other methods. The constrained method exhibits also good X-/S-band agreement with an underestimation in the N_W at the peak of the ray within the range of 20–30 km. Finally, the β method exhibits a good agreement; however, the method also exhibits some weakness in the convective regime where the two profiles show significant differences. In terms of the sensitivity and agreement of the μ parameter, our observation is that the NN and constrained algorithm exhibit good correlation between S- and X-band estimates, particularly in the convective part of the ray, and some overestimation in the weaker regime of the ray. Furthermore, we do not note from this sample ray any effect of deterioration of the X-band versus S-band differences as function of range. These aspects will be further evaluated in the bulk statistics to be discussed next.

In Fig. 5, we show histograms of the XPOL- and S-Pol-estimated DSD parameters (D_0, N_W, and μ) from the three techniques. The figure is a six-panel plot with the left-column panels showing the D_0 retrievals and the right column showing the N_W values. The histograms confirm our observations from the single-ray comparisons shown in Fig. 4. The NN exhibits closer X-/S-band agreements in the distributions of D_0. The constrained method shows an overestimation of the frequency in the range of the larger D_0s, while the β method shows an underestimation of the mode's frequency. In terms of N_W, X-band estimates by NN, β, and constrained methods exhibit similar behavior in their comparison against S-Pol estimates. However, for the NN, there is an underestimation in the mode's frequency with a very good agreement of the β and the constrained method. Namely, the XPOL N_W distribution is flatter relative to the S-Pol, with β method having a tendency to skew toward smaller values, however, exhibits good agreement in the N_W XPOL versus S-Pol distributions. In terms of the mode, we note a shift by about 0.5 toward a higher N_W value for the constrained method, while for the NN, a 34% increase in the frequency of the XPOL relative to S-Pol, and the β method underestimates the tails of the distribution.

Finally, in Fig. 6, we show the rRMSE of XPOL- versus S-Pol-estimated parameters (D_0 and N_W) for different path-integrated-attenuation (PIA) ranges. The points to note from this plot are as follows: 1) there is moderate increase in the XPOL versus S-Pol rRMSE versus PIA, confirming our hypothesis that attenuation correction adds uncertainty in the XPOL retrieval; 2) the constrained method exhibits significant differences between XPOL and S-Pol in the D_0 estimation relative to the other two techniques; 3) both the β and the constrained method perform similar for PIAs less than 30 dBZ in the N_W; and 4) the NN algorithm is the one that performs

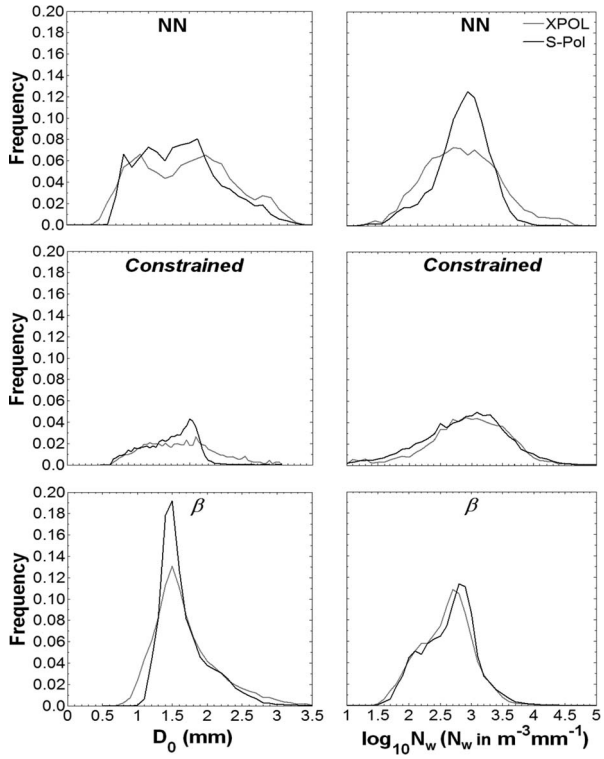

Fig. 5. Frequency histograms of N_W and D_0 parameters estimated by the three DSD retrieval algorithms (NN, constrained, and β) for the corresponding S-Pol and attenuation-corrected XPOL ray profiles.

better with less variability for PIAs less than 35 dBZ, relative to the other methods, in both estimates.

V. Conclusion

This paper presented a comparison of three DSD retrieval algorithms (NN, constrained, and β) based on matched X- and S-band dual-polarization observations and coincident measurements of X-band dual-polarization radar over disdrometer-measured raindrop spectra. The retrieval algorithms, originally developed for C- and S-band polarimetric-radar measurements, were used to estimate the three-parameter "normalized" gamma DSD model.

Specifically, in β method, the slope parameter (β) of a linear axial-ratio model is estimated from the combination of all three polarimetric-radar parameters ($Z_{\rm H}$, $Z_{\rm DR}$, and $K_{\rm DP}$). Parametric relationships are then derived for estimating N_W and D_0 on the basis of β and the other radar parameters. The procedure is founded on simulations with variable β and random distributions of the governing parameters of the gamma DSD that are used to establish relationships with the radar variables $Z_{\rm H}$, $Z_{\rm DR}$, and $K_{\rm DP}$. The constrained method incorporates the $Z_{\rm H}$ and $Z_{\rm DR}$ measurements and an empirical relation between the slope and shape parameters of the DSD as determined from disdrometer measurements. The μ–Λ relation reduces the normalized gamma DSD from three to two independent parameters in that only two radar measurements are required. Axis ratios are assumed constant for the radar-measurement volume. Finally, a nonparametric algorithm based on an *ad hoc* NN technique was devised to estimate the three governing parameters using radar measurements of $Z_{\rm H}$, $Z_{\rm DR}$, and $K_{\rm DP}$. The NN algorithm exhibits the enhanced features to improve its efficiency, robustness, and generalization capability.

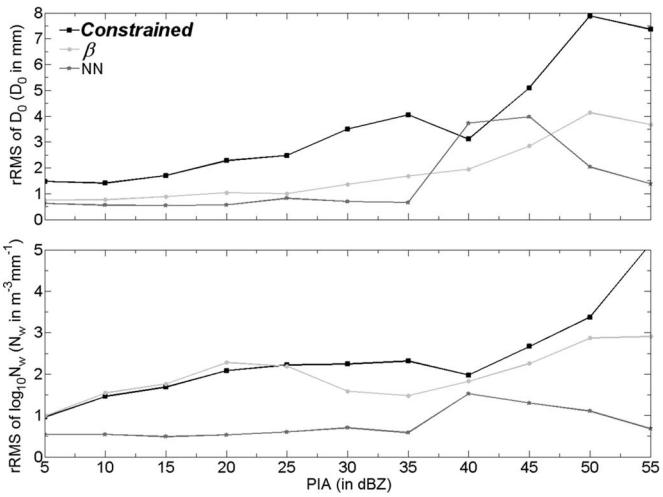

Fig. 6. Relative XPOL/S-Pol rRMSE of (a) median drop diameter D_0 (in millimeters) and (b) the N_W (N_W in $\mathrm{m}^{-3} \cdot \mathrm{mm}^{-1}$) for the three different algorithms (NN, constrained, and β) grouped by ranges of the PIA.

Comparisons of the algorithm retrievals against disdrometer-derived parameters showed that all three algorithms performed well with significant correlations, small biases, and moderate standard errors. The best performance was exhibited by the β and the constrained method, while the NN showed the most sensitivity to radar-measurement error.

The statistics of the DSD-parameter retrievals from the matched XPOL/S-Pol radar rays showed good agreement with high correlations and low systematic differences. In summary, the major disadvantage of the NN and the β methods is that it introduces errors from the use of $K_{\rm DP}$. Furthermore, the use of a linear axis-ratio relation may not be representative of actual raindrop variability, and the power-law fit employed does not guarantee an unbiased estimator with minimum error, because the relations may not capture the true functional form and account for the error distribution [33]. The constrained method avoids the use of simulated axis ratio and the error propagation associated with the use of $K_{\rm DP}$. The procedure works reasonably well at both low and high rain rates and provides relatively accurate retrieval of the DSD parameters. However, additional studies are needed to verify the physical validity of the μ–Λ relation and the stability of the constrained method in different storm types and radar ranges, while the NN method needs to be trained using actual disdrometer raindrop spectra. Finally, S-Pol versus XPOL difference statistics showed low dependence of the retrieval error on PIA, indicating insignificant propagation effect of attenuation-correction uncertainty in the retrieval of the DSD parameters.

Acknowledgment

The MP-X and disdrometer data from Japan were provided by Dr. Maki of the National Research Institute for Earth Science and Disaster Prevention (NIED), Ebina, Japan. X-band dual-polarization radar measurements in IHOP were obtained

with the National Observatory of Athens transportable X-band Dual-Polarization and Doppler radar (XPOL). The S-Pol data from IHOP were provided by NCAR.

REFERENCES

[1] M. N. Anagnostou, E. N. Anagnostou, and J. Vivekanandan, "Correction for rain path specific and differential attenuation of X-band dual-polarization observations," *IEEE Trans. Geosci. Remote Sens.*, vol. 44, no. 9, pp. 2470–2480, Sep. 2006.

[2] M. N. Anagnostou, E. N. Anagnostou, J. Vivekanandan, and F. L. Ogden, "Comparison of raindrop size distribution estimates from X-band and S-band polarimetric observations," *IEEE Geosci. Remote Sens. Lett.*, vol. 4, no. 4, pp. 601–605, Oct. 2007.

[3] D. Atlas and C. Ulbrich, "Drop size spectra and integral remote sensing parameters in the transition from convective to stratiform rain," *Geophys. Res. Lett.*, vol. 33, no. L16, L16 803, Aug. 2006. DOI: 10.1029/2006GL026824.

[4] P. Barber and C. Yeh, "Scattering of electromagnetic waves by arbitrarily shaped dielectric bodies," *Appl. Opt.*, vol. 14, no. 12, pp. 2864–2872, Dec. 1975.

[5] E. A. Brandes, G. Zhang, and J. Vivekanandan, "Experiments in rainfall estimation with a polarimetric radar in a subtropical environment," *J. Appl. Meteorol.*, vol. 41, no. 6, pp. 674–685, Jun. 2002.

[6] E. A. Brandes, G. Zhang, and J. Vivekanandan, "Drop size distribution retrieval with polarimetric radar: Model and application," *J. Appl. Meteorol.*, vol. 43, no. 3, pp. 461–475, Apr. 2004.

[7] V. N. Bringi, V. Chandrasekar, and R. Xiao, "Raindrop axis ratios and size distributions in Florida rainshafts: An assessment of multiparameter radar algorithms," *IEEE Trans. Geosci. Remote Sens.*, vol. 36, no. 3, pp. 703–715, May 1998.

[8] V. N. Bringi, G.-J. Huang, V. Chandrasekar, and E. Gorgucci, "A methodology for estimating the parameters of a gamma raindrop size distribution model from polarimetric radar data: Application to a squall-line event from the TRMM/Brazil campaign," *J. Atmos. Ocean. Technol.*, vol. 19, no. 5, pp. 633–645, May 2002.

[9] R. Doviak and D. S. Zrnic, *Doppler Radar & Weather Observations*, 2nd ed. New York: Academic, 1993.

[10] E. Gorgucci, G. Scarchilli, V. Chandrasekar, and V. N. Bringi, "Rainfall estimation from polarimetric radar measurements: Composite algorithms immune to variability in raindrop shape-size relation," *J. Atmos. Ocean. Technol.*, vol. 18, no. 11, pp. 1773–1786, Nov. 2001.

[11] E. Gorgucci, V. Chandrasekar, V. N. Bringi, and G. Scarchilli, "Estimation of raindrop size distribution parameters from polarimetric radar measurements," *J. Atmos. Sci.*, vol. 59, no. 15, pp. 2373–2384, Aug. 2002.

[12] E. Gorgucci, V. Chandrasekar, and V. N. Bringi, "Drop size distribution retrieval from polarimetric radar measurements," in *Proc. 2nd Eur. Conf. Radar Meteorol.*, Delft, The Netherlands, 2002, pp. 134–139.

[13] E. Gorgucci, V. Chandrasekar, and L. Baldini, "Microphysical retrievals from Dual–Polarization radar measurements at X-band," *J. Atmos. Ocean. Technol.*, vol. 25, pp. 729–741, 2008.

[14] E. Gorgucci, V. Chandrasekar, and L. Baldini, "Microphysical retrievals from dual polarized radar measurements at X-band," in *Proc. 33rd Conf. Radar Meteorol.*, Cairns, Australia, 2006.

[15] M. Maki *et al.*, "Semi-operational rainfall observations with X-band multi-parameter radar," *Atmos. Sci. Lett.*, vol. 6, no. 1, pp. 12–18, Jan. 2005.

[16] J. S. Marshall and W. M. K. Palmer, "The distribution of raindrops with size," *J. Meteorol.*, vol. 5, no. 4, pp. 165–166, Aug. 1948.

[17] S. Y. Matrosov, K. A. Clark, B. E. Martner, and A. Tokay, "X-band polarimetric radar measurements of rainfall," *J. Appl. Meteorol.*, vol. 41, no. 9, pp. 941–952, Sep. 2002.

[18] S. Y. Matrosov, D. E. Kingsmill, B. E. Martner, and F. M. Ralph, "The utility of X-band polarimetric radar for continuous estimates of rainfall parameters," *J. Hydrometeorol.*, vol. 6, no. 3, pp. 248–262, Jun. 2005.

[19] D. N. Moisseev, V. Chandrasekar, C. M. H. Unal, and H. W. J. Russchenberg, "Dual-polarization spectral analysis for retrieval of effective raindrop shapes," *J. Atmos. Ocean. Technol.*, vol. 23, no. 12, pp. 1682–1695, Dec. 2006.

[20] D. N. Moisseev and V. Chandrasekar, "Examination of the $\mu-\Lambda$ relation suggested for drop size distribution parameters," *J. Atmos. Ocean. Technol.*, vol. 24, no. 5, pp. 847–855, May 2007.

[21] D. N. Moisseev and V. Chandrasekar, "Nonparametric estimation of raindrop size distributions from dual-polarization radar spectral observations," *J. Atmos. Ocean. Technol.*, vol. 24, no. 6, pp. 1008–1018, Jun. 2007.

[22] S.-G. Park, V. N. Bringi, V. Chandrasekar, M. Maki, and K. Iwanami, "Correction of radar reflectivity and differential reflectivity for rain attenuation at X band. Part I: Theoretical and empirical basis," *J. Atmos. Ocean. Technol.*, vol. 22, no. 11, pp. 1621–1632, Nov. 2005.

[23] B. E. Sheppard, "Effect of irregularities in the diameter classification of raindrops by the Joss–Waldvogel disdrometer," *J. Atmos. Ocean. Technol.*, vol. 7, no. 1, pp. 180–183, Feb. 1990.

[24] P. I. Joe, "Comparison of raindrop size distribution measurements by a Joss–Waldvogel disdrometer, a PMS 2DG spectrometer, and a POSS Doppler radar," *J. Atmos. Ocean. Technol.*, vol. 11, no. 4, pp. 874–887, Aug. 1994.

[25] J. Sun, "Initialization and numerical forecasting of a supercell storm observed during STEPS," *Mon. Weather Rev.*, vol. 133, no. 4, pp. 793–813, 2005.

[26] J. Testud, E. Le Bouar, E. Obligis, and M. Ali-Mehenni, "The rain profiling algorithm applied to polarimetric weather radar," *J. Atmos. Ocean. Technol.*, vol. 17, no. 3, pp. 332–356, Mar. 2000.

[27] E. Torlaschi and I. Zawadzki, "The effect of mean and differential attenuation on the precision and accuracy of the estimates of reflectivity and differential reflectivity," *J. Atmos. Ocean. Technol.*, vol. 20, no. 3, pp. 362–371, Mar. 2003.

[28] C. W. Ulbrich, "Natural variations in the analytical form of the raindrop size distribution," *J. Appl. Meteorol.*, vol. 22, no. 10, pp. 1764–1775, Oct. 1983.

[29] C. W. Ulbrich and D. Atlas, "Rainfall microphysics and radar properties: Analysis methods for drop size spectra," *J. Appl. Meteorol*, vol. 37, no. 9, pp. 912–923, Sep. 1998.

[30] G. Vulpiani, F. S. Marzano, V. Chandrasekar, A. Berne, and R. Uijlenhoet, "Polarimetric weather radar retrieval of raindrop size distribution by means of a regularized artificial neural network," *IEEE Trans. Geosci. Remote Sens.*, vol. 44, no. 11, pp. 3262–3275, Nov. 2006.

[31] C. R. Williams, A. Kruger, K. S. Gage, A. Tokay, R. Cifelli, W. F. Krajewski, and C. Kummerow, "Comparison of simultaneous rain drop size distributions estimated from two surface disdrometers and a UHF profiler," *Geophys. Res. Lett.*, vol. 27, no. 12, pp. 1763–1766, 2000.

[32] M. Xue, V. Droegemeir, and V. Wong, "The Advanced Regional Prediction System (ARPS)—A multi-scale nonhydrostatic atmospheric simulation and prediction model. Part I: Model dynamics and verification," *Meteorol. Atmos. Phys.*, vol. 75, no. 3, pp. 161–193, Nov. 2000.

[33] A. J. Illingworth and T. M. Blackman, "The need to represent raindrop size spectra as normalized gamma distributions for the interpretation of polarization radar observations," *J. Appl. Meteorol.*, vol. 41, no. 3, pp. 286–297, Nov. 2002.

Marios N. Anagnostou (S'01–M'04) received the B.S. and M.Eng. degrees in electrical engineering from York University, York, U.K., and the Ph.D. degree in environmental engineering from the University of Connecticut, Storrs.

He is currently a Contractor Research Associate with the Institute for Inland Waters, Hellenic Center for Marine Research, Anavissos, Greece. His main research experience and interests are in rainfall microphysics and precipitation remote sensing on the basis of new radar remote-sensing systems such as X-band dual polarization (polarimetric). He has participated in numerous international field experiments, deploying mobile dual-polarization radar. Lately, he has been involved in underwater acoustics for quantitative estimation of rain and wind. He has authored or coauthored more than 13 journal papers in the areas of dual polarization, radar rainfall estimation, and hydrometeorological applications.

Emmanouil N. Anagnostou received the B.S. degree in civil and environmental engineering from the National Technical University, Athens, Greece, and the M.S. and Ph.D. degrees from the University of Iowa, Iowa.

He is currently the Team Leader of a Marie Curie Excellence Team with the Institute of Inland Waters, Hellenic Center for Marine Research, Anavissos, Greece, and an Associate Professor with the Department of Civil and Environmental Engineering, University of Connecticut, Storrs. His current research is on precipitation estimation from space and ground-based sensors and the optimum assimilation of remote sensing data in atmospheric and hydrological models for the prediction of floods and other hydrological variables.

Dr. Anagnostou is a member of the Precipitation Constellation Subgroup, International Committee on Earth Observation Satellites, and of NASA's International Precipitation Science Team. He is the recipient of several prestigious awards, including the 1999 NASA Earth Sciences Directorate New Investigator Award, the 2002 NSF Geosciences Program CAREER Award, and the 2003 Outstanding Junior Faculty Award by the School of Engineering of the University of Connecticut. He is also the recipient of two top-level international awards: the 2002 EGU Plinius Medal for outstanding achievements in the field of natural hazards and important interdisciplinary activity involving remote sensing and hydrometeorological research areas and the 2005 Marie Curie Excellence Award in recognition to pioneering work on precipitation remote sensing and his innovations in multisensor global rainfall measurement.

Gianfranco Vulpiani (M'06) received the Laurea degree in physics and the Ph.D. degree in radar meteorology from the University of L'Aquila, L'Aquila, Italy, in 2001 and 2005, respectively.

In 2001, he was with the Department of Physics and the Center of Excellence CETEMPS, University of L'Aquila, where he was a Research Scientist on ground-based radar meteorology, with special focus on C-band applications and polarimetric applications. He was a Visiting Scientist with Colorado State University, Fort Collins, in 2004. In 2006, he was with the Department of Observation Systems, Météo–France, Paris, France, where he was a Postdoctoral Researcher. Within the framework of the European project FLYSAFE, he has worked on the development of dual-polarization retrieval techniques with a special focus on attenuation correction and hail detection. Since March 2007, he has been with the Department of Civil Protection, Rome, Italy, where he is in charge of the managing the Italian radar network. He is a Reviewer for several international journals in remote-sensing topics.

Mario Montopoli received the Laurea degree in electronic engineering from the University of L'Aquila, L'Aquila, Italy, in 2004. He is currently working toward the Ph.D. degree in radar meteorology in a joint program between the University of Basilicata, Potenza, Italy, and the University of Rome "La Sapienza," Rome, Italy.

In 2005, he joined the Center of Excellence (CETEMPS), University of L'Aquila, as a Research Scientist on ground-based radar meteorology, with a special focus on C-band applications and processing techniques. Since 2006, he has been a Research Assistant with the Department of Electrical Engineering and Information, University of L'Aquila.

Frank S. Marzano (S'89–M'99–SM'03) received the Laurea degree (*cum laude*) in electrical engineering and the Ph.D. degree in applied electromagnetics from the University of Rome "La Sapienza," Rome, Italy, in 1988 and 1993, respectively.

After being a Lecturer with the University of Perugia, Perugia, Italy, in 1997, he joined the Department of Electrical Engineering and cofounded the Center of Excellence (CETEMPS), University of L'Aquila, L'Aquila, Italy, where he is currently the Vice Director. Since 2005, he has been with the Department of Electronic Engineering, University of Rome "La Sapienza," where he currently teaches courses on antennas and remote sensing. He has authored more than 70 papers on international refereed journals and more than 120 extended abstracts in conference proceedings. His current research concerns passive and active remote sensing of the atmosphere from ground-based, airborne, and spaceborne platforms, with a particular focus on precipitation using microwave and infrared data, development of inversion methods, radiative transfer modeling of scattering media, and radar meteorology issues. He is also involved on radio-propagation topics in relation to incoherent wave modeling, scintillation prediction, and rain fading analysis along satellite microwave links.

Dr. Marzano is a member of the Italian Society of Electromagnetics (SIEM). He was the recipient of the 1993 Young Scientist Award of the Twenty-Fourth General Assembly of the International Union of Radio Science and of the 1998 Alan Berman Publication Award from the Naval Research Laboratory, Washington, DC. Since 2001, he has been the Italian National Delegate for the European Cooperation in the Field of Scientific and Technical Research (COST) Action 720 on atmospheric profiling by ground-based remote sensing and Action 280 on satellite fade mitigation techniques. Since January 2004, he has been acting as an Associated Editor of the IEEE GEOSCIENCE REMOTE SENSING LETTERS. In 2004 and 2006, he was a Co-Guest Editor of the Special Issues on MicroRad for the IEEE TRANSACTIONS ON GEOSCIENCE AND REMOTE SENSING.

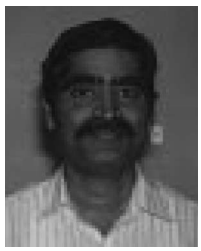

Jothiram Vivekanandan received the B.E. degree in electronics and communications engineering from the Madurai-Kamaraj University, Madurai, India, the M.Tech. degree in microwave and radar engineering from the Indian Institute of Technology, Kharagpur, India, and the Ph.D. degree in electrical engineering from the Colorado State University, Fort Collins, in 1986.

He is currently a Scientist with the National Center for Atmospheric Research, Boulder, CO. His research experience includes microwave radar and radiometer/satellite remote sensing of the atmosphere, vegetation, and soil. He has devoted considerable effort toward modeling polarimetric radar and multifrequency radiometer observations in clouds and their interpretations. He has participated in a number of field programs that involved radar, aircraft, satellite, and ground-based instruments.